

Robust Reversible Data Hiding Algorithm for Color Image Based on 2D-DCT

Qiu-Yu Zhang, Qi-Yan Dou, Rui-Hong Dong, Yan Yan

School of Computer and Communication
Lanzhou University of Technology
Gansu, Lanzhou, 730050, P. R. China

zhangqylz@163.com; 1147025638@qq.com; dongrh@lut.cn; yanyan@lut.cn

Received July, 2016; revised January, 2017

ABSTRACT. *Aiming at the problems such as the poor performance of anti-rotation attacks of reversible data hiding algorithm for color image, and the acerb contradictory between the amount of embedded data and the quality of image perception, a novel reversible data hiding (RDH) algorithm for color image based on two-dimensional discrete cosine transform (2D-DCT) was proposed in this paper. Firstly, for the separation of RGB color channel, the correlation among three color components of RGB and human visual system were used in the proposed algorithm. Secondly, the secret information were embedded into the region by a vector, it is embedded into the host image of low frequency regions using the 2D-DCT, which was not easy to suffer attacks. Finally, the embedded capacity was improved by the pixel complementary algorithm. While the receiver is extracting the secret information, the original cover image can be recovered by the 2D-DCT inverse transformation without any losses. Experimental results show that the proposed algorithm has good robustness and it also has a better ability of anti-rotation, anti-nose and anti-shear attacks, etc. Furthermore, the adaptive selection of embedded capacity has been achieved, when the capacity reached to 1.396 bpp, the average value of PSNR was still higher than 39.185 dB.*

Keywords: Reversible data hiding (RDH), Color image, Two-dimensional discrete cosine transform (2D-DCT), Pixel complementation, High embedded capacity

1. Introduction. The emergence of data hiding technology has greatly enhanced the security of multimedia information [1]. Compared with the data hiding technology, RDH technology can restore both the secret data and the original image of the receiver [2]. With the RDH technology developing mature gradually, its applications are becoming more and more extensive and have played important roles in many fields [3], such as satellite and military image, medical image, two-dimensional engineering graphics. In addition, the existing RDH technology can not fully meet the actual requirements, especially in the face of the color cover image of the different formats and the hacker's wanton destruction. Therefore, studying on the robust and mainly composed of color images RDH technology has very important significance [1-3].

At present, most RDH algorithms are based on lossless compression, histogram shifting and difference expansion [4-7]. Li et al. [8] proposed a RDH scheme for color image based on prediction-error expansion and cross-channel correlation. In his method, the edge of the color image is used to embed secret information. Visual quality of Li's scheme is high

and capacity is high too. Ma et al. [9] proposed a scheme which is based on histogram shifting and embedding data onto image by reversibly vacating room. Mohammed et al. [10] proposed a new robust binary image embedding algorithm in discrete wavelet domain, this algorithm has a certain robustness. Visual qualities of Ma and Mohammed scheme are high but the capacity is low. Khan et al. [11] proposed a novel joint data hiding using adaptive pixels value difference. In their scheme, edge pixels and smooth pixels are used in the adaptive difference expansion method and their capacity is higher than Ma and Mohammed. Pan et al. [12] proposed a RDH scheme based on local histogram shifting with multilayer embedding. The main idea of Pan's method is keeping the histogram peak as reference pixels unchanged, using similar pixels value to embed the secret information, without using the key information of the peak point, finding peak point directly from the histogram and extracting the secret information through the peak point. Multi-embedding is used in embedding process and the embedding capacity of this algorithm is very perfect, but the change of histogram is obvious. Lee et al. [13] proposed An adjustable and RDH method based on multiple-base notational system without location map, the main feature of the algorithm is the use of multiple-base Notational system to replace the location map, and achieve the adaptability of the embedded capacity. Qu et al. [14] proposed a method that extended the traditional channel-dependent payload partition schemes and extremely improved the time efficiency. But there are no more details about adaptive embedding. In addition, Zhang et al. [15] proposed a recursive histogram modification method, established the equivalent between RDH and lossless data compression. Chang et al. [16] proposed a RDH algorithm, the cover image classified into the embeddable block or non-embeddable block in his algorithm. Non-embeddable blocks remain unchanged and embeddable blocks are used to generate two histograms, the addition and subtraction operations were used respectively on two histogram. Therefore, Chang's algorithm is very effective to avoid underflow/overflow problems. In 2016, Weng et al. [17-18] proposed two reversible watermarking algorithms, and the experimental results show that these two algorithms are effective. Rabie and Kamel [19] proposed a global-adaptive-region discrete cosine transform approach. This algorithm has high embedded capacity, but the PSNR value is not high, and has not an ability to resist the attack. The common drawback in all algorithms mentioned above is that they did not take into account the performance of robustness against geometric attacks or the robustness is too poor. What's more, many algorithms above have the problem that the contradiction between the embedding capacity and the perceived quality can not be alleviated.

From what has been discussed above, in order to improve the robustness and the image perceived quality of the RDH algorithm for color images, especially the ability against rotation attacks and select the embedding capacity adaptively, this paper uses the 2D-DCT transformed from pixel complementary algorithm to present a robust RDH algorithm for color image. The two-dimensional DCT transform and inverse transform is applied to the original image in this algorithm, which is more suitable for the embedding secret information of the color image. Under larger embedding capacity premises, the visual effect of the image steganography are better, and in the transmission process the algorithm has certain robustness, the receiver can recover the original image and the secret information without distortion. Experimental results show that the proposed algorithm can balance the contradiction between the embedded capacity and the image quality.

The remaining part of this paper is organized as follows. Section 2 describes related algorithm principle. The detailed robust RDH algorithm for color image is described in Section 3. Section 4 gives the experimental results and performance analysis as compared with other related methods. Finally, we conclude our paper in Section 5.

2. Problem Statement and Preliminaries.

2.1. Two-dimensional DCT Transform and Inverse Transform. DCT, which is based on orthogonal transformation in real number field and avoided the complex number operations of the Fourier transform, not only has good energy compression and the ability to remove correlation, but also has fast algorithms. 2D-DCT algorithm, which is proposed on the basis of one dimensional DCT, conducts a one-dimensional transform on the basis of the one-dimensional transform, so the orthogonal transformation does not change entropy value of the source, and there is no loss of the image information before and after the transformation. Thus the original image can be obtained by inverse transformation absolutely.

Supposing the size of a two dimensional digital image $f(x, y)$ is $M \times N$. The 2D-DCT of the $M \times N$ matrix is defined in Eq. (1):

$$F(u, v) = c(u)c(v) \sum_{x=0}^{M-1} \sum_{y=0}^{N-1} f(x, y) \cos \frac{(2x+1)u\pi}{2M} \cos \frac{(2y+1)v\pi}{2N} \quad (1)$$

The 2D-DCT inverse transform is defined in Eq. (2):

$$f(x, y) = c(u)c(v) \sum_{x=0}^{M-1} \sum_{y=0}^{N-1} F(u, v) \cos \frac{(2x+1)u\pi}{2M} \cos \frac{(2y+1)v\pi}{2N} \quad (2)$$

where $F(u, v)$ represents the coefficients after 2D-DCT transform, $0 \leq x \leq M-1, 0 \leq y \leq N-1, 0 \leq u \leq M-1, 0 \leq v \leq N-1, c(u)$ and $c(v)$ are transform parameters, and the values are as follows:

$$c(u) = \begin{cases} \frac{1}{\sqrt{M}} & u = 0 \\ \sqrt{\frac{2}{M}} & 1 \leq u \leq M-1 \end{cases}, \quad c(v) = \begin{cases} \frac{1}{\sqrt{N}} & v = 0 \\ \sqrt{\frac{2}{N}} & 1 \leq v \leq N-1 \end{cases}$$

Compared with the traditional 2D-DCT, the 2D-DCT transform used in this paper do a certain amount of change. Firstly, full consideration of the transformation effect and perceived quality of the stego image made the 4-by-4 blocks achieve better results than results of image divided randomly. Our method is using two-dimensional transform directly, it is not divide the 2D-DCT into two one-dimensional DCT in turn, so the method is more suitable for color images. After the 2D-DCT transform, it only quantizes the smaller coefficients with coarse level, and retains the coefficients that contain the main information of the image, which is used to compressing code. Moreover, the 2D-DCT compression coding method can not only save a lot of storage space, but also increase the capacity of embedded secret information indirectly. In addition, the 2D-DCT transforms and inverse transform algorithm ensure that the stego image during transmission can resist geometric attacks.

2.2. Pixel Complementary Algorithm. Pixel complementation, also known as pixel compensation, executes first plus 1 minus 1 operation loop if the embedded pixel value is greater than 1 in the two consecutive shift operations. If the embedded pixel value is an even number, the number of the operations plus 1 equal to number of the operations minus 1. If the embedded pixel value is equal to 1, the operation plus 1 will only be performed. If the embedded pixel value is an odd number, the number of the operations plus 1 is more than the operation minus 1. Because of the pixel complementary, the pixel values remain unchanged. So maximizing the use of such a pixel complementarity principle can effectively reduce the embedding distortion caused by circular embedding. Broadly speaking, the pixel complementation means that the effects brought about by

different embedding offset each other after many embedding processes, so that the final pixel value close to or even equal to the original pixel value. For instance, for a given pixel $x_{i,j}$, when the pixel is embedded twice, there will be a pixel complementary phenomenon after modification:

$$x_{i,j}^k - x_{i,j} \leq x_{i,j}^{k-1} - x_{i,j} \quad (3)$$

where $x_{i,j}^k$ represents the pixel valued after k ($k \geq 2$) times to embed, it shows that $x_{i,j}^k$ is more closer to the original pixels than $x_{i,j}^{k-1}$.

In this paper, since the pixel complementary measures have been taken before the reducing of perceived quality, so it is possible to maintain a high PSNR values in the data hiding of larger embedded capacity.

3. Proposed RDH Scheme for Color Image. Firstly, the three color channels are divided into blocks on the basis of the separation of three color channels original RGB. Using 2D-DCT transform, the secret information of the vector are transformed into a color channel according to the complementary way of each element pixel, it is stored point by point, and it can be embedded with loop operations. Finally, by the 2D-DCT inverse transform, we can reconstruct the three color original RGB channels, and combine the three color channels into a color image, and then the stego image is obtained. The whole transmission process has good robustness, it can resist several attacks such as shearing, noise, rotation and so on. In this paper, the principle diagram of RDH algorithm for color image is shown in Fig. 1.

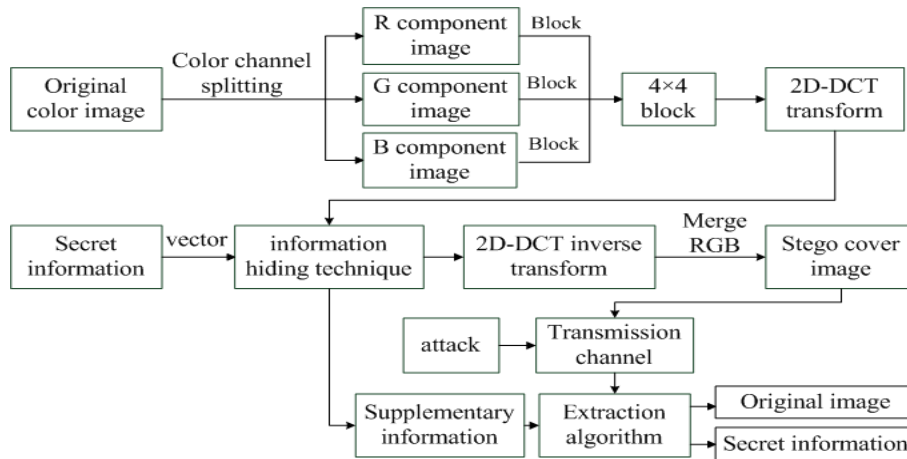


FIGURE 1. The principle diagram of RDH algorithm.

3.1. Data Hiding Procedure. The embedding steps are as follows:

Step 1: Isolate the three color components of color cover image C for IR(red), IG(green), IB(blue). The basic principle is that when the separation of a component, the remaining two color components will be set to zero. The principle is as follows:

Red channel: $IR(:, :, 2) = 0; IR(:, :, 3) = 0;$ % Set green and blue component to zero

Green channel: $IG(:, :, 1) = 0; IG(:, :, 3) = 0;$ % Set the red and blue components to zero

Blue channel: $IB(:, :, 1) = 0; IB(:, :, 2) = 0;$ % Set the red and green components to zero

Step 2: The separated images IR, IG, IB are divided into 4-by-4 blocks. It is divided into non-overlapping blocks (NB), the original image size is $N \times N$ and the size of the block is $L \times L$. The formula for the block can be defined as follows:

$$NB = \left\lfloor \frac{N \times N}{L^2} \right\rfloor \quad (4)$$

where $\lfloor \cdot \rfloor$ represents the under rounding. For instance, the size of the original cover image is 512×512 , the size of the block is 4×4 , thus $NB = \lfloor (512 \times 512)/4^2 \rfloor = 16384$, it means that it can be divided into 16384 non-overlapping blocks.

As a result, all images can be viewed as sequences of small planes, which are determined by a number of important features:

$$F = \bigcup_{i=1, \dots, K} f_i \quad (5)$$

where F represents an image, f_1 represents a small picture or a small plane, K is called the total number of the small image blocks, and $K = 16384$, these images blocks should satisfy the condition of Eq. (6).

$$f_i \cap f_j = \phi \quad (6)$$

where $i \neq j$.

Step 3: In order to protect the original cover image better, so that it can resist attacks and obtain robustness better. Here, weighting processing for each non-overlapping block (NB) according to Eq. (7).

$$NB_g = (1 + \alpha) * NB \quad (7)$$

where NB_g represents the non-overlapping blocks after weighting process, α is called the weighting factor.

Then 2D-DCT transform are performed for each IR in non-overlapping blocks NB_g by the Eq. (1): $DB=2D-DCT(NB_g)$. For embedding secret information, the dimension of secret information (Ec) must be less than the dimension of the cover image. Depending on the size of the secret information, we can decide whether to use IB and IG or not. If the embedded secret information is larger than the set threshold T' , the 2D-DCT transform should be performed for IB. If the capacity of the confidential information is greater than 2 times of the T' , in order to embed all the secret information, the 2D-DCT transforms also should be performed for IG.

Step 4: The secret information picture is converted to vector $\mathbf{a}(\mathbf{k})$ (The secret information (Ec) can be transformed into one-dimensional array), which is prepared to embed into the cover image.

$$\mathbf{a}(\mathbf{k}) = Ec(i, j) \quad (8)$$

Step 5: The low frequency region is selected to embed $\mathbf{a}(\mathbf{k})$ by a Zig-zag scanning way. Because the low frequency domain is not easy to be attacked, it can improve the robustness of the algorithm. Firstly, IR is chosen to embed, if Ec is too large, IB and IG can be chosen to embed the information. The d is the direction of embedded information. The pixel complementary way is adopted in the process of embedding, and it is stored one by one point, so that the embedding capacity of three components RGB reached the maximum, meanwhile the perceived quality won't decline obviously. When each pixel is embedded once, the number of secret information will add 1, mean $count = count + 1$, then it loops over the data. The embedded position e is also embedded into the cover image, and the block image DBC after embedding is obtained according to the formula $DBC = \beta \times \mathbf{a}(\mathbf{k})$, where β presents the weighting factor. As auxiliary information, d and e also are embedded into the cover image, which takes up very little space. Even if the attacker know the auxiliary information, don't know the specific case of embedding algorithm, it is impossible to extract secret information.

Step 6: The Eq. (2) is used to perform the 2D-DCT inverse transform into each DBC : $IDBC = IDCT2(DBC)$, then combining with the three color components, and obtained the secret vector image S . S can resist shear, noise and rotation of any angle during the transmission process.

3.2. Data Extraction and Restoring Procedure. The main task of the recipient are to extract $\mathbf{a}(\mathbf{k})$ and restore the color image of the original cover image. The extraction process is the inverse operation of embedding, and the specific procedures are as follows:

Step 1: The stego image S is divided into IR, IB and IG using the same method of embedding secret information, and then divided them again. And the direction of embedded d and embedded position e is determined according to the auxiliary information.

Step 2: Judging the position of each non-overlapping block NB , and to determine whether the current position is embedded secret information, if not, under a judgment $x = x + 1$. If the secret information is embedded, extract the secret information and count as 1, else count as 0.

Step 3: Judging the embedded direction of the secret information, and determining whether it is positive ($d=-1$) or reverse ($d=1$) and the number of embedded times for each point. If the number of embedding is greater than 2, the pixel complementary approach will be adopted.

Step 4: The vector $\mathbf{a}(\mathbf{k})$ is calculated according to the formula $\mathbf{a}(\mathbf{k}) = (1/\beta) \times DBC$, whenever an extraction is over, the number of secret information will be added 1, namely $count = count + 1$. Then continue to extract the next location of the secret information, and repeat **Step 2** to **Step 4** until all the secret information is extracted.

Step 5: The original cover image construction, the formula $DB' = IDCT2(NB)$ is used to perform the 2D-DCT inverse transforms into each non-overlapping block NB . Each DB' will be combined with a complete map, and the separated IR, IG, IB channel will be merged. Finally, the original cover image C is restored.

4. Experimental Results and Analysis. In this part, experimental hardware platforms are: Inter Core i3 CPU, 350 M, 4 G, 2.27 GHz, Experimental environment is the MATLAB R2012a and Windows 7 operating system. We employ four standard 24 bit color images, from complex to smooth, were selected as the testing images of the resolution of 512×512 pixels as shown in Fig. 2(a). We took random color images as secret information.

We adopted peak signal to noise ratio (PSNR) as measurements of image quality and used embedding bits per-pixel (bpp) as metric to evaluate embedding capacity, where:

The bpp is an index to evaluate the embedded capacity. The greater the value of bpp is, the higher the embedding capacity is. The definition of bpp is as follow:

$$bpp = \frac{\text{Hidden data bits}}{\text{total pixels}} \quad (9)$$

$PSNR$ is the objective evaluation standard of image quality between the cover image and the stego-image. The higher value of $PSNR$ is, the better of image quality is. The equation of $PSNR$ is as follow:

$$PSNR = 10 \log_{10} \left[\frac{MAXPIX}{MSE} \right] \quad (10)$$

where MSE is obtained by using the Eq. (11):

$$MSE = \frac{1}{M \times N} \times \sum_{i=1}^M \sum_{j=1}^N (C(i, j) - S(i, j))^2 \quad (11)$$

$MAXPIX$ is the maximum pixel value which is 255^2 , MSE is mean square error between the cover image C and the stego image S .

This paper carries out a detailed experiment and analysis of attacks on the rotation, shearing, Gaussian Noise, also embedding capacity and image quality, thus proves the superiority of the proposed algorithm.

4.1. Image Quality of the Stego Image and Embedding Capacity Analysis.

The experimental method is as follows: For the same cover image, the secret information are embedded in different capacity and same capacity respectively, and then we find the perceived quality changes of the image. The experimental result indicated that our method has a greater embedding capacity, and when the embedding capacity is large, the perceived quality is also very good, and the performance is stable too.

As shown in Fig. 2(a), four different formats of color images(Airplane.jpg, Lena.bmp, Peppers.tiff, Baboon.jpg) are selected as the original cover image C . Fig. 2(b) is corresponding to Fig. 2(a), it is the stego image S after embedding the secret information.



FIGURE 2. The cover image before and after data hiding.

In order to reflect the superiority of the proposed algorithm, the images of Lena, Peppers, Airplane and Baboon are compared with the results in Wang [4], Huang [7], Li [8] and Ma [9] method. As shown in Fig. 3.

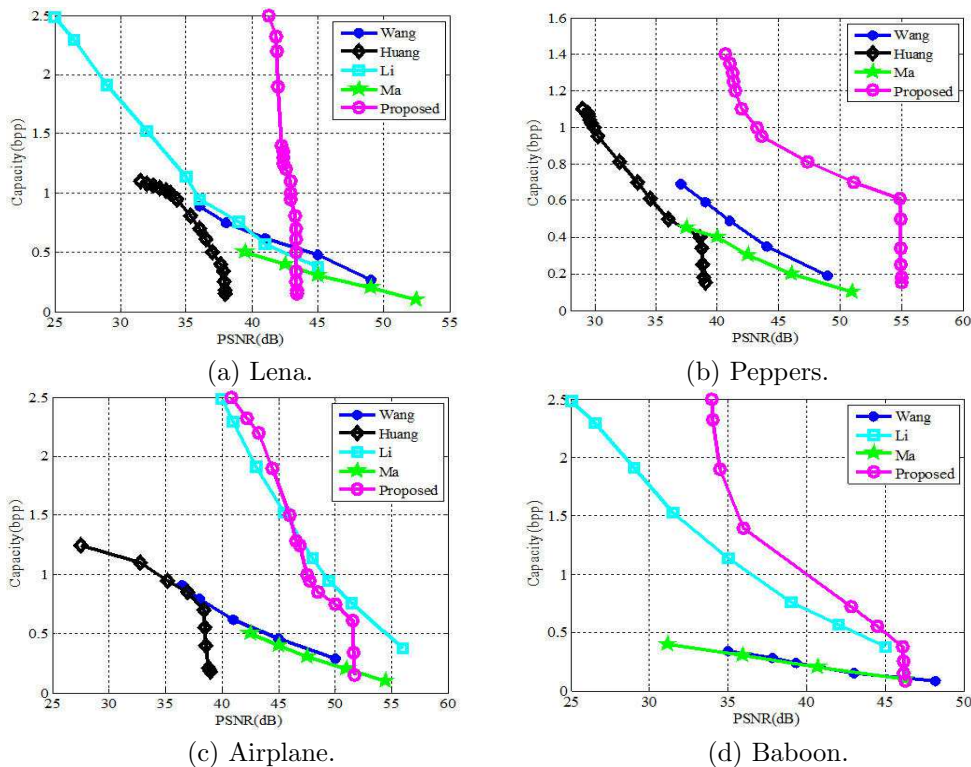


FIGURE 3. Comparison of the embedded capacity with other algorithm.

The proposed algorithm is more suitable for the secret information embedding with the high capacity, and all of the embedding capacities are above 1.0 bpp, which are larger than the results in [4], [7], [8] and [9] method, and the value of $PSNR$ is greater too. For the high capacity of secret data hiding, our method is more stable, and the image quality is better. Besides, there is no obvious distortion by using our method.

The performance of the proposed algorithm is compared with the methods that in Wang [4], Nikolaidis [6] and Huang [7], and the comparison results are shown in Table 1.

TABLE 1. The $PSNR$ value of embedding in different capacities secret information

Cover image	Wang [4]		Nikolaidis [6]		Huang [7]		Our method	
	Payload	$PSNR$	Payload	$PSNR$	Payload	$PSNR$	Payload	$PSNR$
Lena	58982	36.00	45038	39.90	297533	31.68	302500	43.47
Peppers	45875	36.50	52579	38.60	288358	29.00	302500	40.67
Baboon	22937	35.00	76946	32.10	-	-	327680	37.51
Airplane	58982	36.00	-	-	331874	28.30	353894	45.85

As shown in Table 1, our method is better than the algorithm proposed by Nikolaidis method in terms of both embedded capacity and $PSNR$ value, which shows that our method has better stability in secret information embedding with the high capacity.

4.2. Robustness Analysis. As shown in Fig. 4(a), the Lena images are subjected to Gaussian Noise attacks of variance $V=0.0001$, shear attacks and attacks with a counter clockwise rotation of 45° of image. Fig. 4(b) is the restored picture after attack.

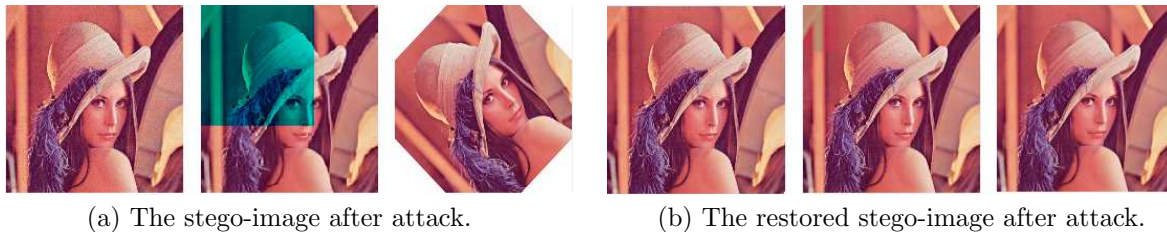


FIGURE 4. The stego-image before and after attack.

In order to verify the robustness of the algorithm, some attack experiments and the contrast experiment are carried out. Table 2 lists $PSNR$ values of different color cover image which is subjected to noise attack, shear attack and rotation attack.

TABLE 2. The $PSNR$ value of same embedding capacities suffering from different attacks

Cover image	Capacity (bpp)	$PSNR$ (dB) after the attack		
		Gaussian Noise	Shearing	Rotation
Airplane	1.396	46.213	51.629	40.839
Lena	1.396	46.276	42.918	41.261
Baboon	1.396	46.206	59.201	33.973
Peppers	1.396	46.476	54.903	40.673

As shown in the Table 2, although the ability to resist rotation attack is weak compared with noise attack and shear attack, the lowest $PSNR$ value can also reach 33.973 dB, and the average value can reach 39.187 dB. For complex texture images, the ability to resist

rotation attacks is weaker than other attacks, but the ability to resist shear attack is still strong. As can be seen from the Table 2, the average *PSNR* of four different texture images after noise attack is 46.293 dB, the average *PSNR* after shearing attack is 52.163 dB, the average *PSNR* after rotation attack is 39.187 dB.

Table 3 is the robustness analysis experiment result when the block size is not the same.

TABLE 3. The Robustness analysis of different block size

Blocks	Attacks	Airplane	Lena	Baboon	Peppers
2×2	Gaussian Noise	47.234	47.289	47.168	54.312
	Shearing	51.773	42.926	60.214	46.393
	Rotation	40.880	41.404	34.337	40.413
4×4	Gaussian Noise	50.518	50.717	49.456	50.580
	Shearing	51.773	42.926	60.213	55.041
	Rotation	42.114	42.383	34.483	42.082
8×8	Gaussian Noise	46.213	46.276	46.206	46.476
	Shearing	51.629	42.918	59.201	54.903
	Rotation	40.839	41.261	33.973	40.673
16×16	Gaussian Noise	46.171	46.264	46.188	46.439
	Shearing	51.551	42.911	59.244	46.337
	Rotation	40.821	41.251	33.966	37.907
32×32	Gaussian Noise	46.183	46.233	46.188	46.410
	Shearing	51.479	42.903	59.116	46.308
	Rotation	40.784	41.228	33.962	37.890

As can be seen from the Table 3, When the block size is 4×4 , the robustness is the best, and with the increase of the block size, the robustness is getting worse. Although the robustness of 2×2 is better than other blocks (8×8 , 16×16 , 32×32), its security is not high, this is because the stego image appeared serious distortion (as shown in Fig. 5) when block is 2×2 , so the secret information is easy to find for attackers, and when the block size is 2×2 , the running speed is very slow in this algorithm. From this, the 4×4 block size used in this paper is proposed, which is not only fast, but also more robust than others.

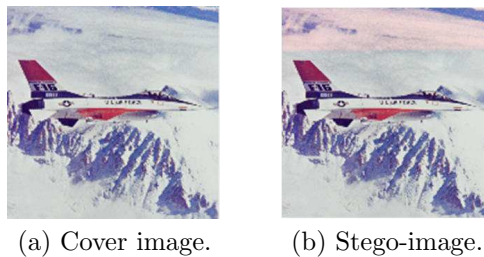


FIGURE 5. The cover image and stego-image when the block size is 2×2 .

The image blocks are weighted to guarantee the stability of the image of our method, and the secret information is embedded in low frequency region, therefore when the arbitrary rotation angle is obtained, the angle rotational alignment can be performed according to the corresponding, and any angle rotation attack can be achieved. In order to further evaluate the performance, the comparison between our method and the Mohammed's[10] method is presented. The Lena images are subjected to Gaussian noise attacks of mean $M=0$, variance $V=0.001$, the same shear attacks and rotation attacks

with a counter clockwise rotation of 45° . The comparison results are shown in Table 4, the ability of our method to resist rotation attack is stronger.

TABLE 4. The *PSNR* value of the Lena image suffering from the same attacks

Attack type	Mohammed [10]	Our method
	<i>PSNR</i> (dB)	<i>PSNR</i> (dB)
Gaussian Noise	29.921	36.518
Shearing	14.465	42.918
Rotation	11.177	35.366

From the above experimental results, it shows that the ability of our method to resist the shear attack of the same embedding rate is the strongest, and the ability to resist noise attacks, rotation attack and other geometric attacks is also better.

The human eye is not sensitive to the blue component, so the embedded information has a good transparency, but the red component has good robustness. Therefore, this paper introduces the algorithm that embedding information in the low frequency region where tends not easy to be attacked, in the red component and in the blue component, so the perceived quality is improved, the robustness against geometric attacks is enhanced too.

4.3. Complexity Analysis. In this paper, the 2D-DCT transform and pixel complementary algorithm are used. The 2D-DCT transform and inverse transform contain many operations, such as the multiplication and addition, and the number of multiplication is less, so the computational complexity is low.

The complexity of pixel complementary algorithm is directly related to the threshold value of T , and the threshold value of T is related to the *PSNR* value. When the *PSNR* value is less than 38 dB, the visual effect of the image will be deteriorated. As shown in Eq. (10) and (11), when the *MSE* value is less than 10.306, the *PSNR* value is greater than 38 dB, all the hidden vector image pixel values S are larger than the original cover image pixel values C , which can ensure good visual effect of the image. Therefore, the threshold value T is 26.

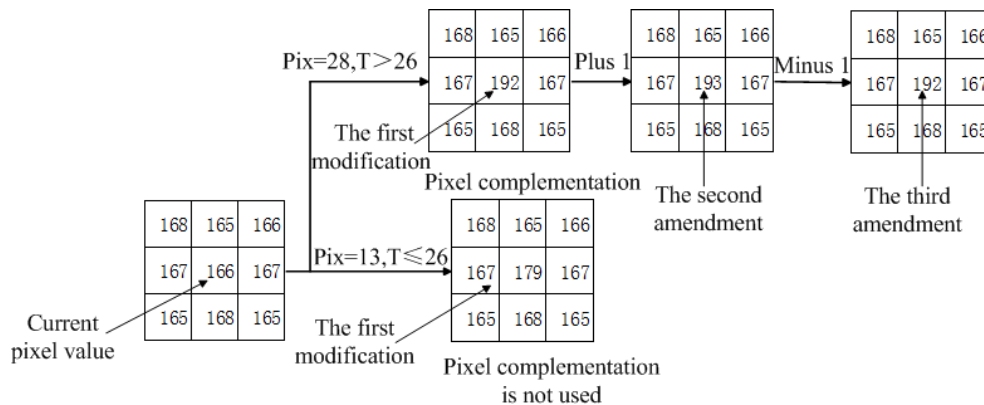


FIGURE 6. The pixel complementary phenomenon of two consecutive embedding.

In this paper, the pixel complementary algorithm processes are shown in Fig. 6, where Pix represents the embedded pixel value, T is the upper threshold of the pixel value. The pixel complementary algorithm is achieved by taking full advantage of multiple cycles.

When the embedded secret information is more than the preset threshold value T , the pixel complementary strategy will be used. When the embedded pixel values $Pix=13$, it is less than the threshold value T , so it will be directly embedded. When the embedded pixel $Pix=28$, it is greater than the threshold values T , so the pixel complementary algorithm will be used. For each pixel beyond the T , execute operation plus 1 first and minus 1 later, all the pixels embedded is completed until the value of total embedded times equals to $Pix-26$. Fig. 6 also shows that the pixel value (192) of the k times is much closer to the value of the original pixel (192) than the pixel value of the $k-1$ (193) times, which can be obtained in the Eq. (3). The whole processes contain simple addition and subtraction operation only, so the complexity of the algorithm is low.

In summary, the complexity of the 2D-DCT transform and pixel complementary algorithm is low.

5. Conclusions and Future Work. In this paper, a robust RDH algorithm for color image is proposed. The algorithm is based on the two-dimensional DCT (2D-DCT) algorithm, which uses the vector method to embed secret information. Since it combines the correlation between pixel complementary and three color components RGB, when embedding the secret information, all of the three color components can be embedded. So the algorithm has a greater embedding capacity and better image quality. Not only the common cover image selection can be realized, but also the embedding capacity adaptive selection can be achieved according to the user requirements, which is more convenient for the user to find the cover image with appropriate size and characteristics to transfer secret information which will not be founded by the attacker. The algorithm does not choose the high frequency region which is vulnerable to attack when transferring secret information, but choose the low frequency region which is not vulnerable to be attacked. Therefore, even in the process of transmission, the stego image can resist rotation, shearing, noise and other attacks. And the receiver can also restore the original image and the secret information without distortion according to the 2D DCT inverse transform.

Next, the research work will study how to improve the performance of the embedding capacity as much as possible on the basis of ensuring the security of the secret information.

Acknowledgment. This work is supported by the National Natural Science Foundation of China (No. 61363078), the Natural Science Foundation of Gansu Province of China (No. 1310RJYA004). The authors would like to thank the anonymous reviewers for their helpful comments and suggestions.

REFERENCES

- [1] B. Ou, X.L. Li, Y. Zhao and R.R. Ni, Efficient color image reversible data hiding based on channel-dependent payload partition and adaptive embedding, *Signal Processing*, vol. 108, pp. 642-657, 2015.
- [2] Y. Q. Qiu and L. Yu, Expanded Generalized Integer Transform Based Lossless Information Hiding Method, *Journal of Electronics and Information Technology*, vol. 37, no. 12, pp. 2830-2837, 2015.
- [3] Z. C. Wang, X.H. Zhao, H. Wang and G.Z. Cui, Information hiding based on DNA steganography, *Proc. of the 2013 4th IEEE Int. Conf. on Software Engineering and Service Science (ICSESS)*, IEEE, Beijing, China, pp. 946-949, 2013.
- [4] J.X. Wang, J.Q. Ni and J.W. Pan, A high performance multi-layer reversible data hiding scheme using two-step embedding, *Proc. of the Int. Workshop on Digital Watermarking*, Springer Berlin Heidelberg, pp. 42-56, 2011.
- [5] X. L. Li, W. M. Zhang, X.L. Gui and B. Yang, A novel reversible data hiding scheme based on two-dimensional difference-histogram modification, *IEEE Transactions on Information Forensics and Security*, vol. 8, no. 7, pp. 1091-1100, 2015.
- [6] A. Nikolaidis, Low overhead reversible data hiding for color JPEG images, *Multimedia Tools and Applications*, vol. 75, no. 4, pp. 1869-1881, 2016.

- [7] H.C. Huang and F.C. Chang, Multi-tier and multi-bit reversible data hiding with contents characteristics, *Journal of Information Hiding and Multimedia Signal Processing*, vol. 7, no. 1, pp. 11-20, 2016.
- [8] J. Li, X.L. Li and B. Yang, Reversible data hiding scheme for color image based on prediction-error expansion and cross-channel correlation, *Signal Processing*, vol. 93, no. 9, pp. 2748-2758, 2013.
- [9] K.D. Ma, W.M. Zhang, X.F. Zhao, N.H. Yu and F.H. Li, Reversible Data Hiding in Encrypted Images by Reserving Room Before Encryption, *IEEE Transactions on Information Forensics and Security*, vol. 8, no. 3, pp. 553-562, 2013.
- [10] A. Mohammed, H.H. Maras and E. Elbasi, A new robust binary image embedding algorithm in discrete wavelet domain, *Proc. of the 2014 IEEE 8th Int. Conf. on Application of Information and Communication Technologies (AICT)*, Astana, KAZ, pp. 1-7, 2014.
- [11] K.N. Khan, K. Karthick, M. Udayakumar and G. Dheepak, A novel joint data hiding using adaptive pixel value difference, *Int. J. Eng. Res. and Sci. and Tech.*, vol. 1, no. 2, pp. 244-249, 2015.
- [12] Z.B. Pan, S. Hu, X.X. Ma and L.F. Wang, Reversible data hiding based on local histogram shifting with multilayer embedding, *Journal of Visual Communication and Image Representation*, vol. 31, pp. 64-74, 2015.
- [13] C. F. Lee, C.C. Chang and P.Y. Pai, An adjustable and reversible data hiding method based on multiple-base notational system without location map, *Journal of Information Hiding and Multimedia Signal Processing*, vol. 6, no. 1, pp. 1-28, 2015.
- [14] D. C. Qu, J.S. Pan, S.W. Weng and S.Q. Xu, A novel reversible data hiding method for color image based on dynamic payload partition and cross-channel correlation, *Journal of Information Hiding and Multimedia Signal Processing*, vol. 7, no. 6, pp. 1194-1205, 2016.
- [15] W. M. Zhang, X.C. Hu, X.L. Li and N.H. Yu, Recursive histogram modification: establishing equivalency between reversible data hiding and lossless data compression, *IEEE Transactions on Image Processing*, vol. 22, no. 7, pp. 2775-2785, 2013.
- [16] C.C. Chang, T.C. Lu, G. Horng, Y.H. Huang and T.J. Hsu, Dual-histograms reversible data hiding capable of avoiding underflow/overflow problems, *Journal of Information Hiding and Multimedia Signal Processing*, vol.6, no. 5, pp. 956-967, 2015.
- [17] S.W. Weng and J.S. Pan, Integer transform based reversible watermarking incorporating block selection, *Journal of Visual Communication and Image Representation*, vol. 35, pp. 25-35, 2016.
- [18] S. W. Weng, J.S. Pan and J. H. Deng, Invariability of remainder based reversible watermarking, *Journal of Network Intelligence*, vol. 1, no. 1, pp.16-22, 2016.
- [19] T. Rabie and I. Kamel, High-capacity steganography: a global-adaptive-region discrete cosine transform approach, *Multimedia Tools and Applications*, vol. 75, no. 2, pp. 1-21, 2016.